ABSORPTION STUDIES OF ACIDIC GASES USING DRY FGD WASTES.

Darrell N. Taulbee and Thomas L. Robl
University of Kentucky-Center for Applied Energy Research
3572 Iron Works Pike, Lexington, KY 40511

Keywords: Acid gases, absorption, CO_2, NO_2, H_2S, SO_2, Flue-gas desulfurization or FGD,

ABSTRACT

Utility boilers and tail-gas desulfurization units that utilize limestone-based sorbents to remove sulfur oxides generate ~20 million tons of flue-gas desulfurization (FGD) wastes each year in the U.S.[1] A substantial portion of the Ca in these wastes remains unsulfated (as CaO or $Ca(OH)_2$), particularly in units that produce *dry* wastes. When hydrated, these materials exhibit a strong affinity to absorb acid gases at ambient temperature in proportion to their available-calcium content and particle size. The work reported here is a continuation of previous investigations of CO_2 and H_2S absorption that includes more recent studies with NO, NO_2, and SO_2. The relative affinity for the gases examined thus far is $SO_2 > CO_2 > H_2S$. CH_4 and NO are not absorbed and NO_2 apparently decomposes at first to NO and HNO_3 before eventually being absorbed as calcium nitrate following depletion of hydration water. The role of available calcium and particle size on absorption capacity and mineralogic changes in the wastes during exposure are discussed.

INTRODUCTION.

In recent years, numerous flue-gas desulfurization (FGD) technologies that utilize limestone-based sorbents, such as fluidized-bed combustors (FBC), spray dryers, and wet scrubbers, have been or will be added to existing utility boilers in an effort to satisfy federally-mandated limits on SO_2 emissions. Such units are normally classified as either *wet* or *dry* depending on whether the absorbent is used in an aqueous slurry (wet) or as a dry or hydrated solid. In addition to differences in the proportions of sulfites and sulfates formed during sulfur capture, dry FGD by-products differ from their wet-scrubber counterparts in that a significant portion of the calcium in the dry waste remains unsulfated. The fraction of unreacted Ca, available as lime (CaO) or slaked lime ($Ca(OH)_2$) can be quite high (> 1/2) depending on scrubber design and operation.

When hydrated, dry FGD wastes strongly absorb acid gases at ambient temperature, e.g. CO_2. Further, absorption can be both rapid and near complete. Such a sorbent may have numerous commercial uses such as the removal of CO_2 from natural gas (the focus of a prior study[2]). Further, considering that about 95% of the ~20 million tons of flue-gas desulfurization (FGD) wastes generated annually in the US is discarded in landfills or holding ponds, commercial utilization of FGD wastes could stand to benefit from both a plentiful low-cost raw material as well as a significant savings in disposal.

In our ongoing study, gas absorption has been examined using waste samples generated in four commercial boilers, a Coolside demonstration-plant run[3], and four tests conducted in the Coolside pilot plant.[4] With the exception of a utility-derived fly ash that served as a control, all study samples are dry-FGD materials. In addition to the absorption studies with CO_2, CH_4 and H_2S previously reported, results from tests with NO, NO_2, and SO_2 are reported here.

EXPERIMENTAL.

Details for the most recent round of testing with NO, NO_2, and SO_2 plus a brief description of the reactor system, study samples, and run procedures are presented in the section to follow. The reader is referred to previous manuscripts for additional information on the latter.[2,5,6]

Absorption Reactors. A schematic of the reactor system shown with a pair of 4" x 3/8"-i.d. ss tube reactors as configured for hydrated solids is shown on the left of Figure 1. Essentially the same system was used to measure absorption by aqueous waste slurries except that a pair of 250 mL-capacity gas scrubbers were substituted for the tube reactors (Figure 1-right). It should be noted that due to the high solubility of SO_2 in and the tendency for NO_2 to decompose on contact with water, only tests with hydrated solids were conducted for these two gases.

Samples. A total of 11 waste samples have been used throughout this investigation.[2,5] Nine of the samples are fly ashes, designated with a -FA suffix. The remaining two, designated with a -BA suffix, are bed ashes. A Class F fly ash (L-FA) from a pulverized-coal-combustion (PCC) utility boiler served as a control and was the only non-FGD sample examined. The four fluidized-bed combustion wastes (FU-FA/BA and CC-FA/BA) were derived from circulating or entrained flow units operating on high-sulfur bituminous coal. Two types of dry, post-combustion flue-gas scrubber material were also examined, a spray-dryer ash from an industrial

boiler in the Midwest, and materials from the Coolside duct-injection technology. The Coolside materials include one sample generated in Ohio Edison's 1990 demonstration of the technology at its Edgewater power plant[3] (*CS*) as well as materials from the CONSOL's Coolside pilot plant in Library, PA (PP1-PP4).[4] The major differences in the waste samples with respect to absorption appears to be in the particle size (BA > FA) and the proportions of free lime which ranged from <3% in the L-FA control to ~20% or greater in the FU-FA, FU-BA, CC-BA, and PP4 samples. Because absorption of CO_2 has been reported for all 11 samples in a previous report, tests conducted in this round were limited for the most part to the FU-FA and PP4 which represent the two samples of fly ash with the highest free-lime content.

Run Procedures. All absorption tests were conducted at ambient temperatures. Hydrated samples were obtained by blending distilled water with dry waste under N_2. 0.5-2 g of the hydrated sample and 6 g of Ottawa sand were packed to the absorbent and bypass reactors, respectively. For the slurry tests, ~5 g of dry sample were added to 200 mL of distilled water in a 250-mL gas scrubber. The bypass scrubber contained distilled water only (200 ml).

Gas flow through the reactors was comprised solely of N_2 in the bypass line. Standard-gas blends containing various combinations of CO_2, H_2S, CH_4, and Ar were metered through the absorbent line.[2,5] Standard-gas blends containing 0.509 vol% NO, 3.82 vol% NO_2, or 3.81 vol% SO_2 were used in this round of testing. These blends were either quantitatively combined with high-purity Ar or with a blend of $Ar/CO_2/CH_4$ (30.3/49.6/20.1 vol%) prior to entering the reactor system. Argon was generally included in all blends as a tracer gas.

The exit streams from both the bypass and sample reactors were combined and continuously sampled with a capillary tube connected to the inlet of a VG-quadrupole mass spectrometer (QMS). The QMS was operated in a selected-ion-monitoring mode in which ion intensities for m/e 15-CH_3^+ (for methane), 18-H_2O^+, 20-Ar^{2+}, 28-N_2^+, 30-NO^+, 34-H_2S^+, 40-Ar^+, 44-CO_2^+, 46-NO_2^+, and/or 64-SO_2^+ were recorded at approximately 1-second intervals.

For both reactor configurations, data collection was initiated with the switching valve in the bypass position, i.e., the test-gas stream passing through the sand-packed bypass reactor. After a timed interval, the valve was rotated so that the test-gas stream was switched to the absorbent reactor as the N_2 stream was simultaneously switched to the bypass reactor. Following exposure, the valve was returned to the initial position to reestablish the QMS baseline. At the conclusion of a run, the QMS molecular-ion signal for each gas of interest was ratioed to the Ar-ion signal. The curves described by these ratios were then numerically integrated over the interval of exposure. By comparing these integrals to the test gas/Ar ratios obtained during passage through the bypass bed (before and after valve switch), the fraction of the test gas absorbed was determined. Since gas flows and sample weights are known, absorption could be converted to an absolute basis (standard cubic feet (SCF)/ton of waste. The same procedure was used for those runs in which more than one test gas was passed through the reactor in the same run.

RESULTS

It was shown in prior studies that the absorption of CO_2 required wetting of the dry FGD waste (hydration or slurry formation). For non-wetted samples, absorption proceeded at a prohibitively slow rate.[2,5] This is illustrated in Figure 2 where absorption of CO_2 is observed to increase in a linear manner up to about 25 wt% added water. Further water addition created a mud-like consistency accompanied by a dramatic decline in the apparent absorption capacity. This decline is presumably due to decreased permeability of the hydrated sample preventing gaseous CO_2 from freely entering the sample bed.

Absorption curves are shown in Figure 3 for a hydrated sample (top) and an aqueous slurry (bottom) prepared from PP4. This figure shows CH_4, CO_2, and H_2S response curves as these gases were concurrently passed through the reactor. These plots indicate that CH_4 was not absorbed, H_2S was moderately absorbed, and CO_2 was extensively absorbed. Closer inspection of the absorption curves reveals that the H_2S response rose to greater than baseline levels in both runs as H_2S was passed through the sorbent bed. This implies that some of the H_2S absorbed early in the exposure was displaced by CO_2 as the capacity of the PP4 sample was depleted. The absorption kinetics were more rapid for the hydrated sample than for the aqueous slurry though on an absolute basis, absorption was about twice as great for the latter (~3,800 SCF/t vs ~1,800 SCF/t). It was previously concluded that CO_2 incorporated into the hydrated sample to form calcite whereas absorption by the waste slurry resulted in capture as HCO_3^- ions which remain in solution. Thus, each CaO unit in the hydrated solids could capture one CO_2 molecule to form $CaCO_3$ or lead to the capture of two CO_2 molecules to form aqueous-phase HCO_3^- ions.

CO_2 absorption by waste slurries is plotted as a function of available-calcium content for the 11

study samples in Figure 4. The majority of the samples plot along a straight line with the exception of the two points on the lower right. These two outlyers represent the two samples of bed ash (FU and CC) whereas the other points in Figure 4 represent samples of fly ash. This plot emphasizes the dependency of CO_2 absorption on both available calcium and particle size. That is, the significantly larger particle size of the bed-ash samples as well as potential blockage of particle pores by chemisorbed SO_2 likely limits diffusion of CO_2 to the particle interior.

Tests with NO, NO_2, and SO_2. Absorption curves for NO, NO_2, and SO_2 are shown in Figure 5 as these gases were passed through either an aqueous slurry (NO) or a hydrated sample of PP4 (NO_2/SO_2). CO_2 was blended to the test-gas stream prior to routing to the absorption reactor for all three runs shown in Figure 5. The top plot shows essentially no absorption of NO. Likewise, no significant absorption of NO was measured when this gas was passed through the slurry without CO_2 (not shown) or when passed through a sample of hydrated PP4 (not shown).

The middle plot in Figure 5 shows simultaneous removal of NO_2 and CO_2. Both gases were extensively absorbed immediately after the valve switch to expose mode. However, ~5 min into the exposure, the response curve for CO_2 exceeded its baseline established during bypass mode (before and after exposure). This suggests that CO_2 initially absorbed was displaced as the run proceeded (absorption capacity of the slurry was depleted). Unlike CO_2 which is chemisorbed by portlandite ($Ca(OH)_2$) to form $CaCO_3$, it is not believed that NO_2 is absorbed as such. Rather, it appears to decompose on contact with hydration water to form HNO_3 and NO. This is supported by the NO and H_2O curves shown in the same plot. Immediately after switching to expose mode, the NO_2 signal is lower than that of NO. However, about 40-45 min into the run, the NO_2 response increases above that of NO concurrent with the depletion of H_2O. This is congruent with a decrease in NO_2 decomposition as the hydration water is consumed. HNO_3 ultimately reacts with portlandite to produce H_2O and calcium nitrate hydrate but not until much of the hydration water is depleted. Finally, integration of the CO_2-response curve revealed a net release of CO_2 of ~150 SCF/t. This production of CO_2 likely derives from calcite ($CaCO_3$) inherent to the FGD waste which is attacked by the newly-formed nitric acid (later discussion).

The bottom plot in Figure 5 shows SO_2/CO_2 absorption. Again, CO_2 was initially absorbed but later displaced by SO_2 as the run proceeded. Integration of the absorption curves (60 min interval) indicated an average absorption of ~3,800 SCF/t SO_2 and a net release of ~550 SCF/t CO_2. Again, the released CO_2 is believed to originate from pre-existing calcite in the PP4 sample as indicated by XRD. The calcite peaks were totally absent in the XRD spectra of wastes following exposure to SO_2. At the end of the 60' exposure, absorption of SO_2 and release of CO_2 is essentially complete. In contrast, during exposure to a blend of NO_2/CO_2 (Figure 5b), NO_2 decomposition and CO_2 displacement is not complete despite the fact that essentially the same volumes of NO_2 and SO_2 were flowed through the reactors during these runs. In a single run with SO_2 and NO_2 (w/o CO_2), SO_2 response began to return to baseline well before NO_2 which again exhibited an inverse relation to water availability. Thus, it would appear that SO_2 removal is controlled by the chemistry of the waste sample whereas NO_2 removal seems more dependent on water content.

Changes in mineralogy. X-ray diffraction (XRD) spectra of hydrated-PP4 waste samples are shown in Figure 6. The top plot (Figure 6a) is for a hydrated sample simultaneously exposed to CO_2 and H_2S, the middle spectrum (Figure 6b) is following exposure to NO_2/CO_2, and the bottom (Figure 6c) is following exposure to SO_2/CO_2. A spectrum of a hydrated sample of PP4 that had not been exposed to the test gases is shown in all three plots for comparison (darker lines). In the top plot, the major mineralogic change was depletion of portlandite ($Ca(OH)_2$) and formation of calcite ($CaCO_3$). There is no indication of CaS formation. When H_2S was passed through the sample without CO_2 (not shown), portlandite was again depleted only this time accompanied by the formation of an unidentified mineral with peaks near 9 and 20 (2-theta). The suspected stoichiometry of the unknown is $Ca(OH)_{2-x}(HS)_x$) though this structure is yet to be confirmed.

Again, depletion of portlandite from the parent to the exposed sample can be seen in Figure 6b in which NO_2 and CO_2 were passed through the hydrated sample. Several new peaks appear which are identified as a hydrated form of calcium nitrate. However, in runs aborted prior to water depletion, these peaks were not observed in the exposed sample. This is consistent with the decomposition of NO_2 to NO and HNO_3 since NO would be released and surface adsorbed HNO_3 would not exhibit an XRD pattern. Thus, the absorbed NO_x species must exist as either HNO_3 or in an amorphous structure. It is speculated that at some point during the exposure as water is depleted, the HNO_3 reacts with portlandite to form H_2O and $Ca(NO_3)_2 \cdot 2H_2O$.

Depletion of portlandite from the parent to the exposed sample is again evident in Figure 6c in

which a mixture of CO_2/SO_2 was used. The minor calcite peaks present in the parent are absent in the exposed sample. Several new peaks appear in the exposed sample which, for the most part, can be attributed to hannebachite ($CaSO_3 \cdot 0.5H_2O$). Thus, it appears that SO_2 is mostly incorporated by substitution for the hydroxyl ions in portlandite with some substitution for CO_2 in the inherent carbonates.

SUMMARY

Hydrated FGD wastes exhibit a strong affinity for CO_2, H_2S, and SO_2 ranging upwards of 4,000 SCF/t for SO_2 in tests with the PP4 and FU-fly ash. The relative order of affinity appears to be $SO_2 > CO_2 > H_2S$. NO_2 was found to decompose on contact with the hydrated samples to form NO and HNO_3 with eventual incorporation as hydrated calcium nitrate. Little or no absorption of CH_4 or NO was observed. In tests of CO_2 absorption, absorption capacity was found to be directly related to the available-calcium content and inversely to the particle size of the waste. Further, absorption did not proceed at a significant rate without the addition of water to the dry wastes. XRD analyses showed that exposure of hydrated FGD wastes to CO_2, H_2S, SO_2, and NO_2 resulted in the depletion of portlandite ($Ca(OH)_2$) and subsequent formation of calcite ($CaCO_3$), an unknown mineral, hannebachite ($CaSO_3 \cdot H_2O$), and initially either an amorphous nitrate/nitrite mineral or absorbed HNO_3 followed by formation of $Ca(NO3)_2 \cdot 2H_2O$, respectively.

ACKNOWLEDGEMENT

The authors wish to thank Dr. U. Graham, Dr. R. Rathbone, and M. Gust for assistance with the XRD analyses; G. Thomas, B. Schram, and M. Grider for sample analyses; and K. Baker of Jefferson Gas Transmission for useful discussions. This work was supported in part by the Morgantown Energy Techn. Ctr., USDOE, under Coop. Agreement DE-AC21-91MC28162 (such support does not constitute an endorsement by the USDoE of the views expressed in this manuscript).

REFERENCES.

1. *Coal Combustion Byproduct (CCB); Production & use: 1966-1993. Report for Coal Burning Utilities in the United States.* American Coal Ash Association, *1995*, Alexandria, VA, 68p.

2. Taulbee, D.N., Graham, U., Rathbone, R.F., and Robl, T.L.; *Prepr., ACS Div. of Fuel Chem.*, **1995**, *40, #4*, American Chemistry Society, Washington, DC, 858-862.

3. Kanary, D.A., R.M. Stanick, H.Yoon, et.al., **1990**, Coolside Process Demonstration at the Ohio Edison Company Edgewater Plant Unit 4-Boiler 13. *Proceedings, 1990 SO_2 Control Symposium* 3, EPRI/U.S. EPA, Session 7A,, New Orleans, LA, 19p.

4. Withum, J.A., W.A. Rosenhoover and H. Yoon, **1988** *Proceedings, 5th Pittsburgh Coal Conf.* University of Pittsburgh, 84-96.

5. Taulbee, D.N.; Graham, U.; Rathbone, R.F.; Robl, T.L.; submitted for publication in *Fuel*, anticipated publication, late 1996.

6. Taulbee, D. N., *Prepr., ACS Div. of Fuel Chem.*, **1993**, *38, #1*, American Chemistry Society, Washington, DC, 324-329.

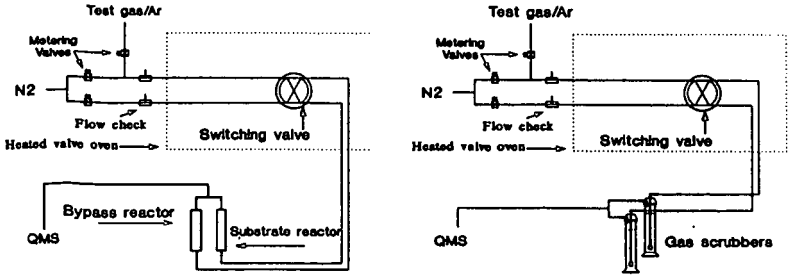

Figure 1. Schematic of the absorption reactors used to measure gas absorption by hydrated-FGD wastes (left) and waste slurries (right).

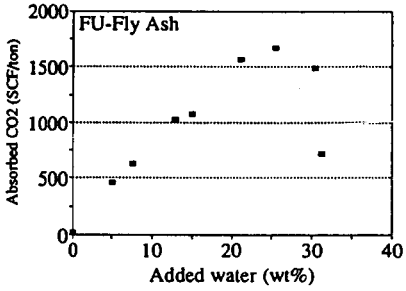

Figure 2. Absorption of CO_2 as a function of prehydration for samples of FU-FA.

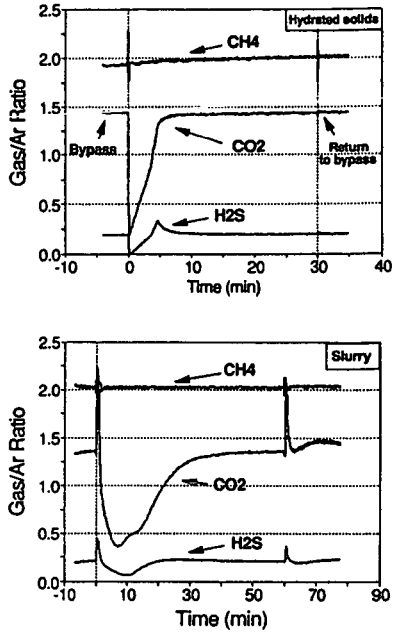

Figure 3. Absorption curves for CH_4, CO_2, and H_2S simultaneously passed through a hydrated sample (top) and aqueous slurry (bottom) of PP4.

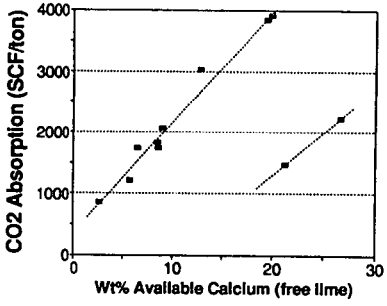

Figure 4. CO_2 absorption as a function of the available calcium. The two points on the bottom right represent samples of bed ash; all others are fly ash samples.

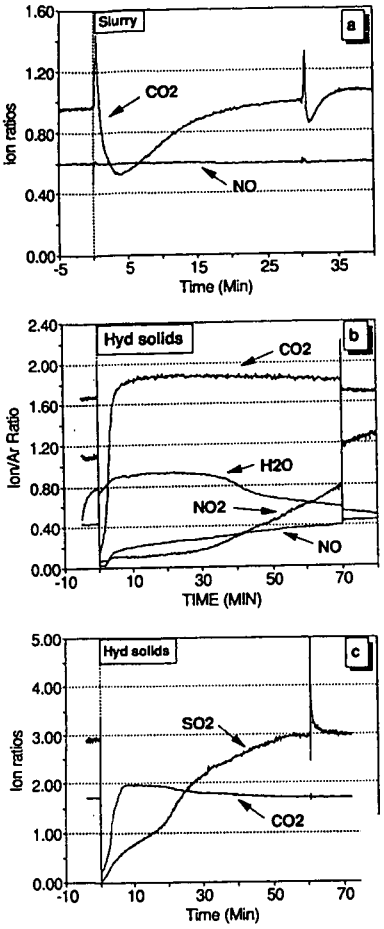

Figure 5. Test gas/Ar ion ratios for NO NO_2 (b), and SO_2 (c) during exposure hydrated PP4 (a) and PP4 slurry (b/c). C absorption shown in all three plots.

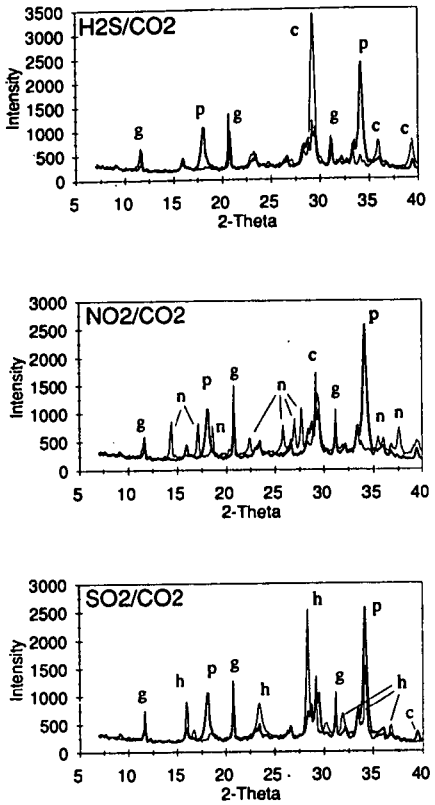

Figure 6. XRD spectra of PP4; hydrated only-darker lines; exposed sample-lighter shading. c-calcite ($CaCO_3$); n-calcium nitrate hydrate; g-gypsum ($CaSO_4 \cdot H_2O$); h-hannebachite ($CaSO_3 \cdot 5H_2O$); p-portlandite-($Ca(OH)_2$).